Techniques in Inorganic Chemistry

Edited by
John P. Fackler, Jr. • Larry R. Falvello

CRC Press
Taylor & Francis Group
Boca Raton London New York

CRC Press is an imprint of the
Taylor & Francis Group, an **informa** business

CRC Press
Taylor & Francis Group
6000 Broken Sound Parkway NW, Suite 300
Boca Raton, FL 33487-2742

Printed in the United States of America on acid-free paper
10 9 8 7 6 5 4 3 2 1

International Standard Book Number: 978-1-4398-1514-4 (Hardback)

Library of Congress Cataloging-in-Publication Data

Techniques in inorganic chemistry / editors, John P. Fackler, Jr., Larry Falvello.
p. cm.
Includes bibliographical references and index.
ISBN 978-1-4398-1514-4 (hardcover : alk. paper)
1. Chemistry, Inorganic--Technique. I. Fackler, John P. II. Falvello, Larry. III. Title.

QD152.3.T434 2011
546.028--dc22 2010019526

Visit the Taylor & Francis Web site at
http://www.taylorandfrancis.com

and the CRC Press Web site at
http://www.crcpress.com

6 Pressure-Induced Change of *d-d* Luminescence Energies, Vibronic Structure, and Band Intensities in Transition Metal Complexes

Christian Reber, John K. Grey, Etienne Lanthier, and Kari A. Frantzen

CONTENTS

Abstract: The effects of hydrostatic pressure on the luminescence spectra of tetragonal transition metal complexes with nondegenerate electronic ground states are analyzed quantitatively using models based on potential energy surfaces defined along normal coordinates. Pressure-induced changes of intensity distributions within vibronic progressions, band maxima, electronic origins, and relaxation rates are discussed for metal-oxo complexes of rhenium(V) and molybdenum(IV) (d^2 electron configuration) and for square-planar complexes of palladium(II) and platinum(II) (d^8 electron configuration).

Keywords: Luminescence spectroscopy, *d-d* transitions, pressure, metal-oxo complexes, square-planar complexes, molybdenum(IV), palladium(II), platinum(II), rhenium(V)

INTRODUCTION

External pressure provides an important pathway to explore the variation of many aspects of solid-state structures, from electrostatic effects to covalent bonds and relatively weak intermolecular interactions, providing an intriguing field for both experimental and theoretical research in a variety of disciplines.[1–3] A large number of pressure-dependent physical properties for many different materials have been reported, as described in a number of extensive reviews with detailed bibliographies covering applications in chemistry, materials science, and physics, as well as the experimental methodology, in particular for spectroscopic measurements.[2–8]

Transition metal complexes are particularly attractive for the study of pressure effects, due to their high-symmetry structures, with many possibilities for subtle variations induced by relatively modest pressures, and their electronic structure, with degenerate and nondegenerate electronic states. Luminescence and absorption spectra of many transition metal compounds, including organometallic molecules, have been measured, and pressure-induced variations have been reported for the energies of their band maxima.[2,4,5,7,8] Excited states with different multiplicities are often close in energy, as illustrated by numerous studies of octahedral chromium(III) complexes, where a pressure-induced emitting state crossover from a quartet to a doublet state has been observed.[7] The corresponding change from a triplet to a singlet emitting state for an octahedral vanadium(III) complex was recently reported.[9] Many literature studies focus on pressure-induced spectroscopic effects caused by ground-state metal-ligand bond length changes, illustrated, for example, by spin-crossover complexes, where pressure can lead to very large metal-ligand bond length changes and even to crystallographic phase transitions.[10,11] Large spectroscopic changes have been observed as a consequence of a few intermolecular effects, involving, for example, the stacking of square-planar d^8 complexes,[12] where pressure-dependent luminescence and triboluminescence phenomena have been compared.[13] Pressure effects on intermolecular distances in luminescent gold(I) cyanides have been reported to lead to significant red shifts of the luminescence maxima due to shorter metal-metal distances.[7,14] A middle ground between intra- and intermolecular effects of pressure is occupied by exchange-coupled polymetallic complexes[6,15,16] and materials of interest as molecular magnets.[17] Phenomena such as piezochromism, mechanochromism, and their characterization through luminescence spectroscopy and other properties, such as electrical conductivity measurements, have been reviewed recently.[18–20] There are many effects where small changes to the environment of transition metal compounds create large changes of their properties, reported as tribochromism[21] and vapochromism.[22,23] Several of the compounds showing these phenomena can be probed by luminescence spectroscopy, and adjustable external pressure provides an important tool to study and control such effects.

This chapter addresses an apparent gap in the literature: On the one hand, structural changes occupy a prominent place in high-pressure research; on the other hand,

the vast majority of literature reports on high-pressure luminescence and absorption spectroscopy focus on band maxima and rationalize the observed variations entirely in terms of electronic energy levels, neglecting effects due to pressure-induced changes of the structural differences between the initial and final states of the transition. The traditional approach allows transitions to be classified based on the pressure-induced shifts of band maxima,[4,5,24,25] but more detailed comparisons have to take into account the vibronic nature of electronic transitions, leading to resolved structure and broad bands for many transition metal compounds. In ambient pressure spectroscopy, often carried out at low temperature, the vibronic spectra obtained with different spectroscopic techniques have been quantitatively analyzed with theoretical models,[26–30] and the chemical and photochemical consequences of excited-state distortions have been discussed.[27,31] Only a small number of recent studies link these two aspects and determine pressure-dependent structural changes between the ground and excited states of transition metal complexes, for example, in octahedral halide complexes of chromium(III)[32] and vanadium(III),[9] where luminescence spectra were used, and in permangante, where pressure-dependent absorption and resonance Raman spectra have been analyzed.[33]

Theoretical work on pressure-dependent electronic spectra is based on potential energy surfaces. Traditionally, assumptions are made that lead to calculated variations of band maxima and widths using quantities that are not obvious to determine experimentally, such as local compressibilities and assumptions on the variation of crystal field parameters with metal-ligand bond distance.[34–36] Most often, experimental results with sufficient detail to determine potential energy surfaces were not available for these studies. Recent work based on electronic structure calculations shows interesting trends for relatively simple transition metal complexes, such as the octahedral VCl_6^{3-} anion,[37] and new general approaches have been described,[38] but not yet applied to transition metal complexes.

In the following, we summarize recent work on the combination of experimental and calculated spectra based on potential energy surfaces defined by adjustable parameters. Resolved vibronic structure is often observed for the examples presented, providing key information for the application of straightforward theoretical models. Two types of tetragonal complexes are explored: first, d^2-configured metal-oxo complexes, and second, square-planar complexes of metal ions with the d^8 electron configuration.

ONE-DIMENSIONAL NORMAL COORDINATE MODEL

The potential energy surfaces for the initial and final states of a transition are a key aspect of any model used to calculate electronic spectra. All examples discussed in the following involve transition metal complexes with nondegenerate electronic ground states, leading to luminescence spectra arising from a transition to a single electronic state. The simplest quantitative model for a luminescence transition involves two harmonic potential energy curves along a single normal coordinate, as illustrated in Figure 6.1. The highest-energy transition in this model is the electronic origin of the luminescence spectrum, denoted as E_{00}. The luminescence band maximum is at E_{max}, also given in Figure 6.1. The potential energy minima are offset by

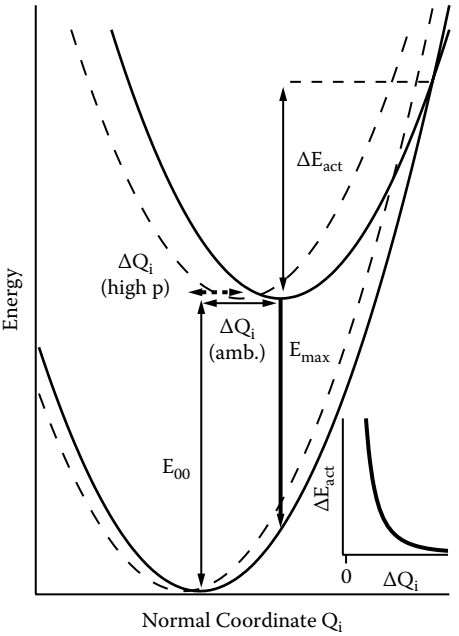

FIGURE 6.1 Potential energy curves at ambient pressure (solid) and at high pressure (dotted) for the ground and emitting states along a single normal coordinate Q_i. The spectroscopic parameters E_{00}, E_{max}, ΔQ_i, and ΔE_{act} are defined. The only change at high pressure is a decrease of ΔQ_i. The inset shows the variation of the activation energy ΔE_{act} with ΔQ_i.

an amount ΔQ_i along the normal coordinate Q_i. The final parameter of interest is the activation energy ΔE_{act}, which, in a simple classical view, determines the nonradiative relaxation rate constant: If it is high, the nonradiative relaxation processes are expected to be inefficient. The change of these four parameters with pressure will be analyzed from luminescence spectra for the transition metal complexes discussed in the following. The only other quantities needed to define the curves in Figure 6.1 are the vibrational frequencies of the mode associated with the normal coordinate Q_i in the ground and emitting states. The ground-state frequencies are found to change by very small amounts from pressure-dependent Raman spectra, and such frequency changes do not have a significant effect on the luminescence spectra.

The model in Figure 6.1 is chosen for a substantial offset ΔQ_i and for a situation where the emitting-state potential energy minimum is at a larger value of Q_i than the ground-state minimum, corresponding to weaker metal-ligand bonds in the emitting state. For this case, it is easy to qualitatively estimate the effect of external pressure on ΔQ_i: Its magnitude is expected to decrease because pressure affects the emitting-state minimum more strongly than the ground-state minimum, as illustrated by the dotted potential energy curves in Figure 6.1. This model therefore corresponds to a complex for which ΔQ_i decreases under high pressure, as indicated in Figure 6.1 by ΔQ_i (high pressure), which is set to a smaller value than ΔQ_i at ambient pressure. In order to obtain the dotted potential energy curves, the value of ΔQ_i was decreased by

9%, a value comparable to the 10% to 15% decreases of offsets ΔQ_i reported in the literature for halide complexes of chromium(III) between ambient pressure and 50 kbar.[32] Changes of the energies E_{00} and E_{max} are also expected with pressure. Their magnitudes and signs depend on the specific bonding situation and will be discussed in the following. The influence of pressure on the activation energy ΔE_{act} is shown in the inset to Figure 6.1: As ΔQ_i decreases, the activation energy increases strongly.

Calculated luminescence spectra for both sets of potential energy curves in Figure 6.1 are shown in Figure 6.2 at high and low resolution. Such calculations are easily carried out for harmonic and anharmonic potential energy surfaces.[26–30] The spectra shown as solid traces correspond to the ambient pressure potential energy curves denoted by solid curves in Figure 6.1. A long progression is observed as a consequence of the large offset ΔQ_i. The members of the progression are separated by the ground-state vibrational frequency of the mode with normal coordinate Q_i, and the intensity distribution within the progression depends strongly on the magnitude of ΔQ_i. Such progressions are observed for many transition metal complexes, most often at low temperature. The decrease of ΔQ_i in Figure 6.1 leads to the spectra shown as dotted traces in Figure 6.2. The energies of the maxima forming the resolved progression are independent of the magnitude of ΔQ_i, as illustrated by the dotted vertical line, but the intensity distribution within the progression changes significantly, showing an increase for the high-energy members of the progression and a decrease for the maxima at lower energy. The change of ΔQ_i with pressure can

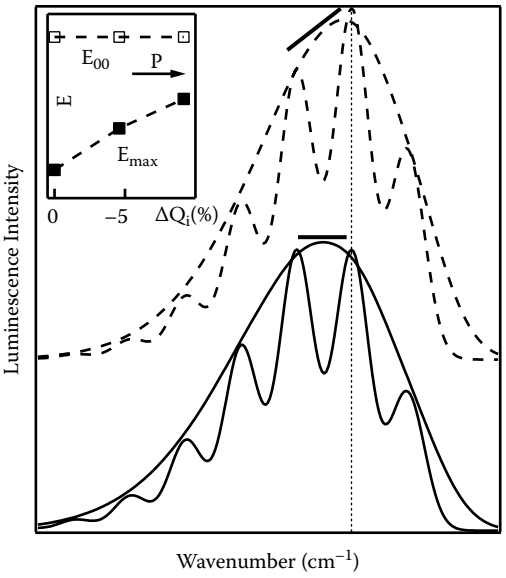

FIGURE 6.2 Luminescence spectra calculated from the potential energy curves in Figure 6.1. Spectra at ambient pressure are given by solid lines, and those at high pressure by dotted lines. The bars above the spectra illustrate the change in vibronic intensities resulting from a decrease of ΔQ_i in Figure 6.1. The inset shows the variation of E_{00} and E_{max} obtained from the calculated spectra.

be determined by fitting calculated spectra, as shown in Figure 6.2, to experimental spectra with resolved vibronic structure. Typically, ΔQ_i and E_{00} are treated as adjustable parameters, defining E_{max} and ΔE_{act}. At lower resolution, only an unresolved band with a single maximum is observed, as illustrated by the low-resolution envelopes in Figure 6.2. The maximum E_{max} of the spectrum at high pressure, shown as a dotted trace, is closer to the vertical dotted line than the maximum of the ambient pressure spectrum, denoted by the solid trace. The decrease of ΔQ_i with pressure is the only modification to any parameter value used to calculate the high-pressure spectra in Figure 6.2. It leads to a blue shift of the luminescence band maximum, as shown in the inset to Figure 6.2. The energy of the electronic origin E_{00} is constant in the high-pressure calculated spectra in the inset of Figure 6.2. The increase of E_{max} indicates that an interpretation of band maxima with pressure in terms of purely electronic models can be fallible: A pressure-induced shift of E_{max} occurs even if the electronic energy difference between the ground and emitting states, defining the electronic origin E_{00}, does not change. Vibronic effects, such as the decrease of the energy difference between E_{00} and E_{max} in the inset of Figure 6.2, need to be considered. The model in Figure 6.1 can be used to obtain quantitative parameter values from experimental spectra, as illustrated in the following.

PRESSURE EFFECTS ON VIBRONIC PROGRESSIONS AND LUMINESCENCE ENERGIES: METAL-OXO COMPLEXES

The luminescence spectra of many different metal-oxo complexes have been reported, and they often show distinct progressions in the metal-oxo stretching mode due to large offsets $\Delta Q_{metal\text{-}oxo}$ between the minima of the potential energy surfaces of the ground and emitting states along the metal-oxo normal coordinate.[39–46] In the following, we discuss the pressure effects on room temperature luminescence spectra of *trans*-dioxo rhenium(V) and mono-oxo molybdenum(IV) complexes, both containing metal centers with a d^2 electron configuration. All spectra were measured using a highly sensitive Raman microscope spectrometer with the 514.5 and 488.0 nm excitation lines of an argon ion laser. A diamond anvil cell was used to control the hydrostatic pressure on the sample crystals, and ruby luminescence was used for pressure calibration. The luminescence bands of the metal-oxo complexes discussed here are in the visible and near-infrared spectral regions and often show a dominant progression involving the metal-oxo stretching mode with a frequency of approximately 900 cm^{-1}.

The highest occupied and lowest unoccupied orbitals of these six-coordinate complexes arise from the t_{2g} orbitals in the O_h point group. The metal-oxo bonds are conventionally used to define the molecular z axis, leading to the occupied d_{xy} orbital (b_{2g} in D_{4h} point group symmetry), lower in energy than the empty $d_{xz,yz}$ (e_g in D_{4h} point group symmetry) orbitals.[39–45] Many complexes with different ancillary ligands in the xy plane show almost identical rhenium-oxo bond lengths of 1.765 Å, varying by only 0.001 Å for *trans*-dioxo complexes of rhenium(V) with ethylenediamine, pyridine, or 1-methylimidazole ligands in the xy plane.[47,48]

Figure 6.3 shows the pressure-dependent luminescence spectra of *trans*-$ReO_2(py)_4I$ and *trans*-$ReO_2(tmen)_2Cl$ at room temperature.[49–51] The abbreviations py

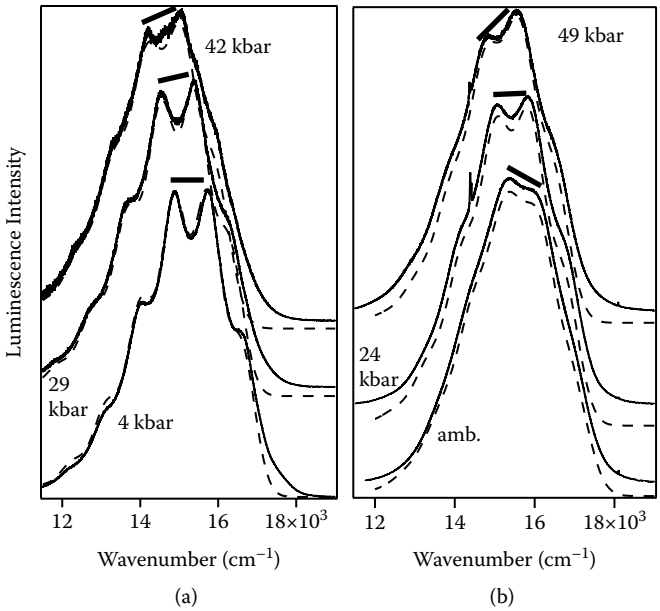

FIGURE 6.3 Experimental (solid lines) and calculated (dotted lines) pressure-dependent luminescence spectra of *trans*-$ReO_2(py)_4I$ (a) and *trans*-$ReO_2(tmen)_2Cl$ (b) at room temperature. Traces are offset along the ordinate for clarity, and all spectra are normalized to identical areas.

and tmen denote pyridine and tetramethylethylenediamine ligands, respectively. The progression in the metal-oxo mode is clearly visible in both spectra. As pressure increases, the intensity distribution within the progression changes toward higher intensities for the members of the progression at high energy. This is the change expected for a pressure-induced decrease in the offset $\Delta Q_{O=Re=O}$ along the metal-oxo coordinate, as discussed in the preceding section and shown in Figure 6.2. The overall change between ambient pressure and approximately 40 kbar is larger for *trans*-$ReO_2(tmen)_2Cl$ than for *trans*-$ReO_2(py)_4I$, as illustrated by the sloping lines above the spectra in Figure 6.3. In addition, a red shift of the entire luminescence band is observed as pressure increases, another consequence of the pressure-induced compression of metal-ligand bonds. The rhenium-nitrogen single bonds are weaker, and therefore more affected by pressure than the metal-oxo double bonds. These large bond length changes lead to stronger electrostatic crystal field changes for the filled d_{xy} orbital involving the metal-nitrogen bonds and to a higher destabilization than for the empty $d_{xz,yz}$ orbitals involved in the metal-oxo double bonds, whose energy is less affected by pressure. In the molecular orbital view, the metal-nitrogen π-antibonding character of the d_{xy} HOMO orbital leads to a strong increase of its energy with pressure, dominating the weaker energy increase of the metal-oxo π-antibonding $d_{xz,yz}$ LUMO orbitals and resulting in a red shift of the luminescence band.

Spectra calculated with one-dimensional potential energy curves along the rhenium-oxo coordinate are shown as dotted lines in Figure 6.3. They reproduce the

TABLE 6.1
Pressure Dependence of Room-Temperature Luminescence Parameters for Metal-Oxo Complexes, Obtained from Fits of Calculated Spectra to Experimental Spectra

Compound	E_{max} (cm^{-1}) ± $\Delta E_{max}/Dp$ (cm^{-1}/kbar)	$\Delta E_{00}/\Delta p$ (cm^{-1}/kbar)	$\Delta Q/\Delta p$ (Å/$kbar^{-1}$)	$\hbar\omega_{metal\text{-}oxo}$ (cm^{-1}) + $\Delta\hbar\omega/\Delta p$ (cm^{-1}/kbar)
$ReO_2(py)_4I$[a]	15,360 – 15.7	–17.6	$-0.6 \cdot 10^{-4}$	905 + 0.53
$ReO_2(tmen)_2Cl$[b,c]	15,590 – 4.6	–8.4	$-1.9 \cdot 10^{-4}$	868 + 0.42
$ReO_2(en)_2Cl$[b,c]	13,780 – 6.8	–12.0	$-2.5 \cdot 10^{-4}$	898 + 0.37
$MoOCl(CN\text{-}t\text{-}Bu)_4BPh_4$[d]	11,950 + 12.0	n/a	≈0[e]	954 + 0.24
$MoOF(py)_4BPh_4$[d]	13,000 – 7.5	n/a	n/a	953 + 0.18

Note: Luminescence band maxima E_{max}, their pressure-induced changes and those of electronic origins E_{00}, offsets ΔQ_i along the metal-oxo stretching normal coordinate, and metal-oxo Raman frequencies are given.

[a] Grey et al.[51]

[b] Grey et al.[50]

[c] Grey et al.[53]

[d] Lanthier and Reber.[54]

[e] Estimated from the spectra in Figure 6.5.

experimental data precisely and lead to a quantitative determination of the parameters E_{00}, E_{max}, and $\Delta Q_{O=Re=O}$ for each pressure at which a spectrum was measured. The variations were found to be linear over the pressure range studied, and the slopes determined for the series of metal-oxo complexes compared here are summarized in Table 6.1. The band maxima E_{max} were determined from the calculated spectra by broadening each vibronic transition, as illustrated for the band envelopes in Figure 6.2. The pressure-induced variations of the parameters are illustrated in Figure 6.4 and show significant differences between these two compounds with similar ambient pressure luminescence properties. The band maxima for *trans*-$ReO_2(py)_4I$ show a much stronger red shift of –15.7 cm^{-1}/kbar than those of *trans*-$ReO_2(tmen)_2Cl$, where a shift of –4.6 cm^{-1}/kbar is obtained. The electronic origins for both compounds show a stronger red shift than the band maxima: –17.6 and –8.4 cm^{-1}/kbar for *trans*-$ReO_2(py)_4I$ and *trans*-$ReO_2(tmen)_2Cl$, respectively. This pressure-induced decrease of the energy difference between E_{00} and E_{max} again corresponds to the expectation for smaller $\Delta Q_{O=Re=O}$ values at high pressure, experimentally defined in the inset to Figure 6.2. This decrease, illustrated by the difference of the slopes for E_{00} and E_{max} in Figure 6.4, is approximately twice as large for *trans*-$ReO_2(tmen)_2Cl$ than for *trans*-$ReO_2(py)_4I$. Both the intensity distributions and the energies obtained from the calculated spectra indicate a decrease of $\Delta Q_{O=Re=O}$ with increasing pressure. The magnitude of this decrease for the two *trans*-dioxo complexes is compared in Figure 6.4b. The slopes differ by a factor of three, and $\Delta Q_{O=Re=O}$ values at 40 kbar are smaller by 7% and 2% than the ambient pressure values for *trans*-$ReO_2(tmen)_2Cl$ and *trans*-$ReO_2(py)_4I$,

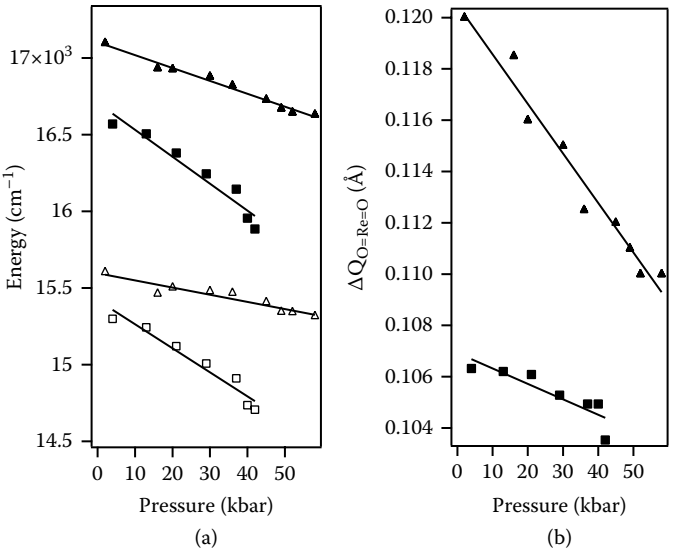

FIGURE 6.4 Pressure-induced variations of luminescence parameters for *trans*-$ReO_2(py)_4I$ (squares) and *trans*-$ReO_2(tmen)_2Cl$ (triangles). (a) Band maxima E_{max} (open symbols) and electronic origins E_{00} (solid symbols), (b) $\Delta Q_{O=Re=O}$. The slopes of the solid lines are given in Table 6.1.

respectively. The larger decrease for *trans*-$ReO_2(tmen)_2Cl$ is qualitatively obvious from the more prominent change in intensity distribution within the progression, illustrated in Figure 6.3 over an identical pressure range for both compounds. A more quantitative analysis of the spectra of *trans*-$ReO_2(tmen)_2Cl$ in Figure 6.3b reveals that the anharmonicity on the long-distance side of the ground-state potential energy curve along the $Q_{O=Re=O}$ normal coordinate is trimmed off by high pressure.[49,50]

The different variations of $\Delta Q_{O=Re=O}$ with pressure for the two complexes in Figure 6.3 can be rationalized qualitatively from the effects of coupling between the ground state and excited states of identical symmetry. This effect is significant for *trans*-$ReO_2(tmen)_2^+$ but small for *trans*-$ReO_2(py)_4^+$.[45,50–52] It has been shown to more strongly influence lower-energy luminescence bands,[45,50] and therefore a larger pressure-induced variation of $\Delta Q_{O=Re=O}$ is expected for complexes such as *trans*-$ReO_2(en)_2^+$, where the pressure-induced decrease of the energy difference between E_{00} and E_{max} is more pronounced than for the *trans*-dioxo complexes with higher-energy luminescence bands in Figures 6.3 and 6.4, leading to a decrease of $\Delta Q_{O=Re=O}$ larger by 25% than for *trans*-$ReO_2(tmen)_2^+$, as summarized in Table 6.1. In addition to the luminescence energy, the size of the offset between ground- and emitting-state potential energy minima along the rhenium-ancillary ligand stretching coordinate also appears to influence the magnitude of the pressure-induced decrease of $\Delta Q_{O=Re=O}$. It is intuitively appealing to assume that large, monodentate ligands, such as pyridine, are more strongly affected by external pressure than compact, chelating ligands such as tetramethylethylenediamine, leading to the stronger red shift for *trans*-$ReO_2(py)_4I$, but this correlation is too simplistic, as a *trans*-dioxo complex

with monodentate imidazole ligands shows a very small red shift of the luminescence band maximum E_{max} by only –2 cm^{-1}/kbar.[53] Pressure-dependent luminescence spectra reveal the important influence of the ancillary ligand, but it is obvious that a larger set of compounds needs to be studied in order to rationalize all observed effects. The comparison of the experimental and calculated luminescence spectra in Figure 6.3 leads to quantitative values for the parameters defining the ground- and emitting-state potential energy curves in Figure 6.3. The pressure-induced variations of $\Delta Q_{O=Re=O}$ and E_{00} or E_{max} are shown to be independent: A larger change of $\Delta Q_{O=Re=O}$ is observed for *trans*-$ReO_2(tmen)_2Cl$ than for *trans*-$ReO_2(py)_4I$, but the inverse order is obtained for the red shifts of E_{00} and E_{max}.

Mono-oxo complexes of d^2-configured metals provide an interesting comparison to *trans*-dioxo compounds. Molybdenum(IV) complexes are illustrative examples with easily discernible Mo-oxo progressions dominating the low-temperature luminescence spectra.[42,43,54] Vibronic progressions in the metal-oxo mode are shorter for mono-oxo compounds than for *trans*-dioxo complexes of both second- and third-row d-block metal ions.[42,43,54,55] Figure 6.5 shows the pressure-dependent luminescence spectra of $MoOCl(CN\text{-}t\text{-}Bu)_4BPh_4$. At ambient pressure and room temperature, the first and second members of the progression in the Mo-oxo modes are visible as a shoulder at approximately 12,700 cm^{-1} and as the overall maximum. Their relative intensities show no pressure-induced variation within experimental accuracy, as indicated by the sloped lines in Figure 6.5, in contrast to the spectra in Figure 6.3, where a change is easily observed. This indicates that the offset $\Delta Q_{Mo\text{-}oxo}$ changes very little over the pressure range in Figure 6.5, an important difference between the *trans*-dioxo and mono-oxo moieties.

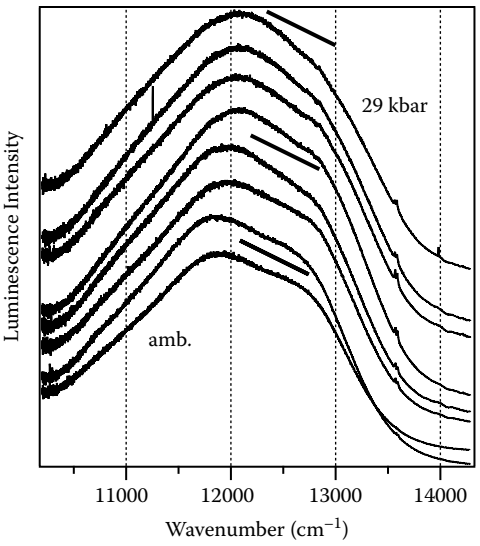

FIGURE 6.5 Pressure-dependent luminescence spectra of $MoOCl(CN\text{-}t\text{-}Bu)_4BPh_4$ at room temperature. The solid bars indicate the negligible variation of the intensity distribution within the vibronic progression in the Mo-oxo vibrational mode.

The band maximum in Figure 6.5 shows a blue shift of +12 cm^{-1}/kbar with pressure, in contrast to all *trans*-dioxo complexes in Figure 6.3 and Table 6.1, where a red shift is observed. This is a consequence of the strong π-acceptor character of the isocyanide ligands. Their π-bonding interactions with the metal d_{xy} orbital lead to a decrease in energy as the Mo-C bonds are compressed. A mono-oxo complex with pyridine ancillary ligands, $MoOF(py)_4BPh_4$, shows a pressure-induced red shift of –8 cm^{-1}/kbar for its band maximum, similar to the *trans*-dioxo complex of rhenium(V) with pyridine ligands.

The overview in this section is intended to illustrate that the predominantly metal-centered *d-d* transitions of metal-oxo complexes are well suited to a detailed exploration of pressure-induced luminescence effects caused by metal-ligand bonds with different characteristics, such as bond orders.

PRESSURE-INDUCED INCREASE OF LUMINESCENCE INTENSITIES AND PRESSURE-TUNED INTERMOLECULAR INTERACTIONS: SQUARE-PLANAR COMPLEXES

Square-planar complexes have long been of interest due to their open coordination sites along the fourfold rotation axis. Both intra- and intermolecular structural effects can be varied through external pressure, as reported recently in detailed variable-pressure structural studies of two-electron redox transformations in square-planar platinum(II) and palladium(II) halides[56] and intramolecular apical and equatorial metal-sulfur interactions in *cis*-[$PdCl_2$(1,4,7-trithiacyclononane)].[57] These studies show that metal-ligand bond lengths decrease by approximately 0.001 Å/kbar, and that changes of distances between a metal center and uncoordinated atoms are significantly larger, as illustrated by the observed decrease of the apical Pd···S distance by 0.005 Å/kbar in *cis*-[$PdCl_2$(1,4,7-trithiacyclononane)] between ambient pressure and 30 kbar.[57] The luminescence properties of square-planar complexes can be varied by slight changes of their environment, such as grinding crystals to a powder.[58] The pressure-dependent luminescence spectra of a variety of square-planar complexes of platinum(II) have been studied.[59–62] In the following, we focus on crystalline complexes with sulfur ligator atoms and *d-d* luminescence transitions. All structures show metal-metal distances longer than 8 Å, and no stacking of luminophores along the z axis, defined as the fourfold axis of the square-planar luminophore, occur.[60,62,63]

The series of complexes compared in the following are $M(SCN)_4^{2-}$ and $M(SeCN)_4^{2-}$, where M denotes palladium(II) and platinum(II). Low-temperature luminescence spectra show rich resolved vibronic structure with progressions involving the totally symmetric M-S stretching modes, as well as the nontotally symmetric stretching mode and the S-M-S bending mode.[60,61,64] The lowest-energy electronic transition from the singlet ground state to a triplet excited state involves the population of the σ-antibonding $d_{x^2-y^2}$ orbital and leads to a large change in metal-ligand bonding, giving rise to the vibronic structure of the luminescence spectra and to an expected blue shift of the luminescence band maximum due to shorter metal-ligand bonds at high pressure. Room-temperature luminescence spectra are shown for $Pd(SCN)_4^{2-}$ in Figure 6.6a. In contrast to the metal-oxo complexes discussed in the preceding section,

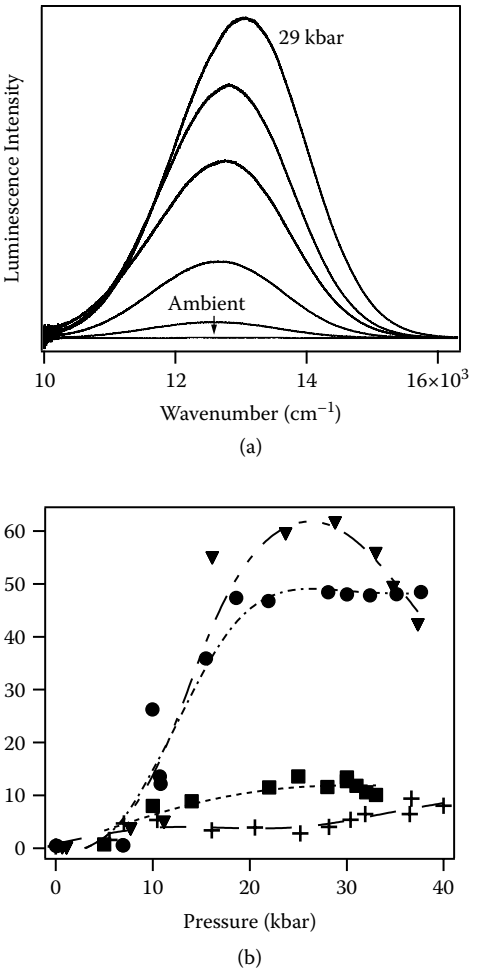

FIGURE 6.6 (a) Pressure-dependent luminescence spectra of $Pd(SCN)_4(n\text{-}Bu_4N)_2$ at room temperature. (b) Pressure-dependent luminescence lifetimes for $Pd(SCN)_4(n\text{-}Bu_4N)_2$ (circles), $Pd(SeCN)_4(n\text{-}Bu_4N)_2$ (triangles), $Pt(SCN)_4(n\text{-}Bu_4N)_2$ (squares), and $Pt(SeCN)_4(n\text{-}Bu_4N)_2$ (crosses).

no vibronic structure is resolved. The band maximum shows a pressure-induced blue shift of +29 cm^{-1}/kbar, similar in magnitude to the shifts observed for octahedral halide complexes of first-row transition metals.[9,32] The most obvious pressure effect is the dramatic increase of the luminescence intensity shown in Figure 6.6a.[61] The ambient pressure luminescence is very weak, and temperature-dependent spectra and lifetimes indicate that nonradiative relaxation processes dominate the excited-state deactivation at room temperature. External pressure leads to more competitive radiative rates, resulting in more intense luminescence. The pressure-dependent luminescence lifetimes in Figure 6.6b for all four compounds in this series show a distinct increase of the lifetime as pressure increases, indicating that nonradiative

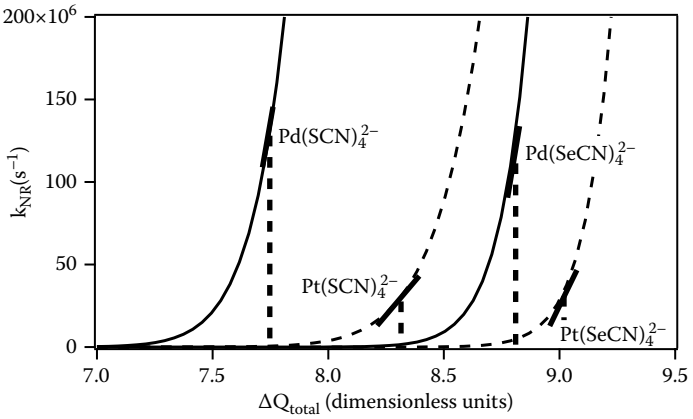

FIGURE 6.7 Variation of the nonradiative relaxation rate constant as a function of total offset between ground- and emitting-state potential energy minima for square-planar complexes.

relaxation rates decrease substantially with pressure.[60] At the highest pressures in Figure 6.6b, intensities and lifetimes decrease, likely due to efficient energy transfer among the closer-spaced complexes to quenching traps or pressure-induced structural imperfections. The increase of both luminescence intensities and lifetimes with pressure appears to be more pronounced for the palladium(II) complexes than for their platinum(II) analogs, as illustrated in Figure 6.6b, a difference that cannot be correlated with other phenomenological quantities, such as the pressure-induced shifts of the luminescence maxima. These shifts are +24 and +29 cm^{-1}/kbar for $Pt(SCN)_4^{2-}$ and $Pd(SCN)_4^{2-}$, respectively, but despite their similar magnitudes, very different enhancements of the luminescence intensities and lifetimes are observed for these two complexes in Figure 6.6b, indicating that the variation of other quantities, in particular the offsets ΔQ_i in Figure 6.1, are of importance.

The schematic view in Figure 6.1 is useful to qualitatively rationalize the pressure-induced decrease of the nonradiative relaxation rate. In the square-planar complexes, a decrease of ΔQ_i along several coordinates is expected as pressure increases, leading to a large increase of the activation energy ΔE_{act}, the classical barrier for nonradiative relaxation. This increase is strongly nonlinear, as illustrated in the inset to Figure 6.1. The ambient pressure offsets ΔQ_i can be determined for all compounds from low-temperature spectra with resolved vibronic structure. These are an important ingredient to models for nonradiative relaxation rates, in addition to vibrational frequencies of the modes associated with these normal coordinates. Temperature-dependent luminescence lifetimes lead to best-fit values for the adjustable parameters of established theoretical models for the nonradiative relaxation rate constants, qualitatively corresponding to the energy barrier ΔE_{act} in Figure 6.1 and the preexponential factor in the classical activation energy picture.[60] From this set of parameters, the variation of the nonradiative rate constant as the offsets ΔQ_i decrease is easily calculated without additional parameters. This variation is shown in Figure 6.7 for the four complexes as a function of the sum of all ΔQ_i values. External pressure

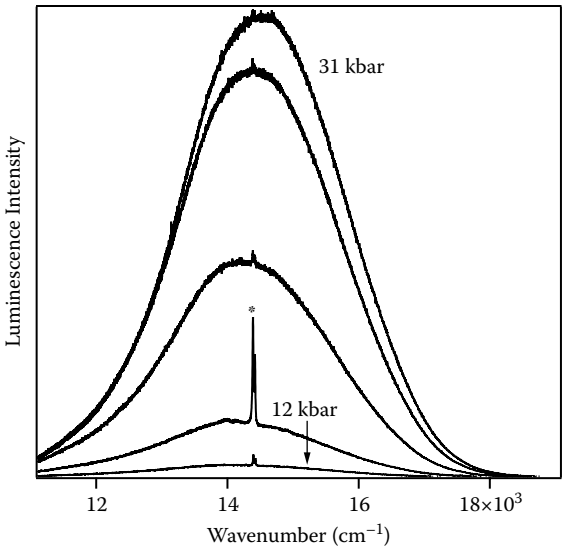

FIGURE 6.8 Pressure-dependent luminescence spectra of Pd(pyrrolidine-N-dithiocarbamate)$_2$ at room temperature. The asterisk denotes ruby luminescence used to calibrate the hydrostatic pressure in the diamond anvil cell.

causes a small decrease of ΔQ_{total}, and the slopes for each complex in Figure 6.7 indicate the magnitude of the variation of luminescence intensities and lifetimes. This simple approach immediately reveals larger slopes for palladium(II) complexes than for their platinum(II) analogs. The pressure-dependent luminescence intensities and lifetimes therefore provide a detailed view on excited-state relaxation, not accessible from ambient pressure data alone, and again emphasizing the importance of the offsets ΔQ_i, whose variation is neglected in purely electronic models.

The influence of individual offsets ΔQ_i on the increases of luminescence intensities and lifetimes still has to be explored in detail for these square-planar complexes. Complexes with chelating ligands are a first step in this direction. Figure 6.8 shows luminescence spectra of the Pd(pyrrolidine-N-dithiocarbamate)$_2$ complex.[65] Its luminescence energy and bandwidth are very similar to those of $Pd(SCN)_4^{2-}$, confirming that it originates from a *d-d* transition. The band maximum shows a blue shift of +13 cm^{-1}/kbar. An obvious increase of the luminescence intensity is observed, but it is less pronounced than for the monodentate ligands in Figure 6.6a. It appears, therefore, that normal coordinates such as S-M-S bending that are blocked by the bidentate ligand play a significant role for the observed pressure effect. The changes in luminescence properties arising through external pressure from intramolecular ground- and emitting-state effects can again be rationalized in the context of the model defined in Figure 6.1.

Intermolecular interactions in square-planar platinum(II) complexes can have a significant influence on the *d-d* luminescence spectrum. An example based on the $[Pt(SCN)_4]^{2-}$ luminophore is shown in Figure 6.9. The trimetallic {$Pt(SCN)_2$[μ-SCN)$Mn(NCS)(bipyridine)_2]_2$} complex has a luminescence maximum and bandwidth

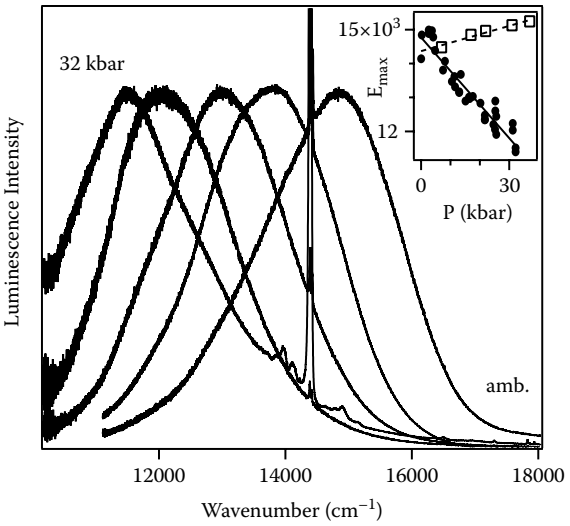

FIGURE 6.9 Pressure-dependent single-crystal luminescence spectra of the trimetallic complex {$Pt(SCN)_2[m\text{-}SCN)Mn(NCS)(bipyridine)_2]_2$}. The inset shows the strong red shift of the band maximum for the trimetallic complex (solid circles and line) compared to the blue shift observed for $Pt(SCN)_4(n\text{-}Bu_4N)_2$ (open squares and dotted line).

similar to those of $Pt(SCN)_4(n\text{-}Bu_4N)_2$ at ambient pressure, but its maximum shows a pressure-induced red shift of –99 cm^{-1}/kbar,[66] in contrast to the blue shift of +24 cm^{-1}/kbar observed for $Pt(SCN)_4(n\text{-}Bu_4N)_2$.[60] These different trends are shown in the inset of Figure 6.9. Neither the magnitude nor the sign of this red shift can be rationalized with the intramolecular effects discussed in the preceding paragraphs. It arises from intermolecular interactions between bipyridine ligands of neighboring complexes and the d_z^2 orbital of the platinum(II) center. The intermolecular distances decrease strongly as pressure increases and influence the molecular electronic states involved in the metal-centered transition in specific structures, such as that of the trimetallic complex in Figure 6.9.[66] Pressure-induced red shifts of the *d-d* luminescence maxima have also been observed for platinum(II) complexes with 1,4,7-trithiacyclononane ligands,[67] illustrating the dominant influence of the decreasing apical Pt···S distance. Comparable red shifts of luminescence band maxima have been reported for other types of emission transitions and arise from metal-metal interactions in stacked structures with metal centers separated by distances on the order of 3 Å at ambient pressure,[12,59] indicative of the variety of interactions that can be probed by pressure-dependent spectroscopy.

CONCLUSIONS

This chapter summarizes how detailed insight on a variety of effects can be gained from pressure-dependent *d-d* luminescence bands. The exploration of such effects has become very accessible, due to sensitive detection with microscope spectrometers combined with established, versatile diamond anvil cells. An interesting direction of

future research is focused on the variation of other relatively weak interactions using luminescence transitions other than the *d-d* bands discussed in this chapter and other spectroscopic techniques, such as resonance Raman measurements. Such studies will most likely require a combination of pressure-dependent spectroscopy and crystallography. Pioneering work in this area has been carried out for salts of $Pt(CN)_4^{2-}$ [12] and $Au(CN)_2^-$,[7,14] but many intriguing pressure effects for compounds outside these two classes of late transition metal compounds remain to be discovered.

ACKNOWLEDGMENTS

Financial support from the Natural Science and Engineering Research Council (Canada) is gratefully acknowledged. We thank Professor Ian S. Butler (McGill University, Montreal, Canada) for encouraging us to measure pressure-dependent spectra, for many helpful discussions, and for the loan of a diamond anvil cell for early measurements.

REFERENCES

1. Grochala, W., R. Hoffmann, J. Feng, and N. W. Ashcroft. 2007. The chemical imagination at work in very tight places. *Angew. Chem. Int. Ed.*, 46, 3620.
2. Drickamer, H. G. 1990. Forty years of pressure tuning spectroscopy. *Ann. Rev. Mater. Sci.*, 20, 1.
3. Hemley, R. J. 2000. Effects of high pressure on molecules. *Ann. Rev. Phys. Chem.*, 51, 763.
4. Drickamer, H. G. 1986. Pressure tuning spectroscopy. *Acc. Chem. Res.*, 19, 329.
5. Drickamer, H. G. 1974. Electronic transitions in transition metal compounds at high pressure. *Angew. Chem. Int. Ed.*, 13, 39.
6. Kenney III, J. W. 1999. Pressure effects on emissive materials. In *Optoelectronic Properties of Inorganic Compounds*, ed. D. M. Roundhill and J. P. Fackler Jr., 231. New York: Plenum Press.
7. Bray, K. L. 2001. High pressure probes of electronic structure and luminescence properties of transition metal and lanthanide systems. *Top. Curr. Chem.*, 213, 1.
8. Grey, J. K., and I. S. Butler. 2001. Effects of high external pressure on the electronic spectra of coordination compounds. *Coord. Chem. Rev.*, 219–221, 713.
9. Wenger, O. S., and H. U. Güdel. 2002. Luminescence spectroscopy of V^{3+}-doped Cs_2NaYCl_6 under high pressure. *Chem. Phys. Lett.*, 354, 75.
10. Gütlich, P., V. Ksenofontov, and A. B. Gaspar. 2005. Pressure effect studies on spin-crossover compounds. *Coord. Chem. Rev.*, 249, 1811.
11. Jeftic, J., C. Ecolivet, and A. Hauser. 2003. External pressure and light influence on internal pressure in a spin-crossover solid $[Zn:Fe(ptz)_6](BF_4)_2$. *High Press. Res.*, 23, 359.
12. Gliemann, G., and H. Yersin. 1985. Spectroscopic properties of the quasi one-dimensional tetracyanoplatinate(II) compounds. *Struct. Bond.*, 62, 87.
13. Leyrer, E., F. Zimmermann, J. I. Zink, and G. Gliemann. 1985. Triboluminescence, photoluminescence, and high-pressure spectroscopy of tetracyanoplatinate salts. Determination of the pressure at triboluminescent sites. *Inorg. Chem.*, 24, 102.
14. Fischer, P., J. Mesot, B. Lucas, A. Ludi, H. H. Patterson, and A. Hewat. 1997. Pressure dependence investigation of the low-temperature structure of $TlAu(CN)_2$ by high-resolution neutron powder diffraction and optical studies. *Inorg. Chem.*, 36, 2791.
15. Riesen, H., and H. U. Güdel. 1987. Pressure tuning of exchange interactions in dinuclear chromium(III) complexes. *Inorg. Chem.*, 26, 2347.

16. Riesen, H., and H. U. Güdel. 1987. Effect of high pressure on the exchange interactions in binuclear chromium(III) complexes. *J. Chem. Phys.*, 87, 3166.
17. Coronado, E., M. C. Giménéz-Lopez, G. Levchenko, F. M. Romero, V. Garciá-Baonza, A. Milner, and M. Paz-Pasternak. 2005. Pressure-tuning of magnetism and linkage isomerism in iron(II) hexacyanochromate. *J. Am. Chem. Soc*, 127, 4580.
18. Takeda, K., I. Shirotani, and K. Yakushi. 2000. Pressure-induced insulator-to-metal-to-insulator transitions in one-dimensional bis(dimethylglyoximato)platinum(II), $Pt(dmg)_2$. *Chem. Mater.*, 12, 912.
19. Takagi, H. D., K. Noda, and S. Itoh. 2004. Piezochromism and related phenomena exhibited by palladium complexes. *Platinum Met. Rev.*, 48, 117.
20. Todres, Z. V. 2004. Recent advances in the study of mechanochromic transitions. *J. Chem. Res.*, 89.
21. Lee, Y.-A., and R. Eisenberg. 2003. Luminescence tribochromism and bright emission in gold(i) thiouracilate complexes. *J. Am. Chem. Soc.*, 125, 7778.
22. Grove, L. J., J. M. Rennekamp, H. Jude, and W. B. Connick. 2004. A new class of platinum(II) vapochromic salts. *J. Am. Chem. Soc*, 126, 1594.
23. Mansour, M. A., W. B. Connick, R. J. Lachicotte, H. J. Gysling, and R. Eisenberg. 1998. Linear chain Au(I) dimer compounds as environmental sensors: A luminescent switch for the detection of volatile organic compounds. *J. Am. Chem. Soc.*, 120, 1329.
24. Drickamer, H. G., and K. L. Bray. 1990. Pressure tuning spectroscopy as a diagnostic for pressure-induced rearrangements (piezochromism) of solid-state copper(II) complexes. *Acc. Chem. Res.*, 23, 55.
25. Moreno, M., J. A. Aramburu, and M. T. Barriuso. 2004. Electronic properties and bonding in transition metal complexes: Influence of pressure. *Struct. Bond.*, 106, 127.
26. Heller, E. J. 1981. The semiclassical way to molecular spectroscopy. *Acc. Chem. Res.*, 14, 368.
27. Zink, J. I., and K.-S. K. Shin. 1991. Molecular distortions in excited electronic states determined from electronic and resonance Raman spectroscopy. *Adv. Photochem.*, 16, 119.
28. Reber, C., and J. I. Zink. 1992. Unusual features in absorption spectra arising from coupled potential energy surfaces. *Comments Inorg. Chem.*, 13, 177.
29. Wexler, D., J. I. Zink, and C. Reber. 1994. Spectroscopic manifestations of potential surface coupling along normal coordinates in transition metal complexes. *Top. Curr. Chem.*, 171, 173.
30. Brunold, T., and H. U. Güdel. 1999. Luminescence spectroscopy. In *Inorganic Electronic Structure and Spectroscopy*, ed. E. I. Solomon and A. B. P. Lever, 259. Vol. I. New York: John Wiley & Sons.
31. Zink, J. I. 2001. Photo-induced metal-ligand bond weakening, potential surfaces, and spectra. *Coord. Chem. Rev.*, 211, 69.
32. Wenger, O. S., R. Valiente, and H. U. Güdel. 2001. Influence of hydrostatic pressure on the Jahn–Teller effect in the $^4T_{2g}$ excited state of $CrCl_6^{3-}$ doped $Cs_2NaScCl_6$. *J. Chem. Phys.*, 115, 3819.
33. Khodadoost, B., S. Lee, J. B. Page, and R. C. Hanson. 1988. Resonance Raman scattering and optical absorption studies of MnO_4^- in $KClO_4$ at high pressure. *Phys. Rev. B*, 38, 5288.
34. Drickamer, H. G., C. W. Frank, and C. P. Slichter. 1972. Optical versus thermal transitions in solids at high pressure. *Proc. Natl. Acad. Sci. USA*, 69, 933.
35. Okamoto, B. Y., W. D. Drotning, and H. G. Drickamer. 1974. The evaluation of configuration coordinate parameters from high pressure absorption and luminescence data. *Proc. Natl. Acad. Sci. USA*, 71, 2671.
36. Moreno, M. 2002. Effects of hydrostatic and chemical pressures on impurities determined through optical parameters. *High Press. Res.*, 22, 29.

37. Seijo, L., and Z. Barandarián. 2003. High pressure effects on the structure and spectroscopy of V^{3+} substitutional defects in Cs_2NaYCl_6. An *ab initio* embedded cluster study. *J. Chem. Phys.*, 118, 1921.
38. Cruz, S. A., and J. Soullard. 2004. Pressure effects on the electronic and structural properties of molecules. *Chem. Phys. Lett.*, 391, 138.
39. Winkler, J. R., and H. B. Gray. 1983. Emission spectroscopic properties of dioxorhenium(V) complexes in crystals and solutions. *J. Am. Chem. Soc.*, 105, 1373.
40. Winkler, J. R., and H. B. Gray. 1985. Electronic absorption and emission spectra of dioxorhenium(v) complexes. Characterization of the luminescent ^3E_g state. *Inorg. Chem.*, 24, 346.
41. Miskowski, V. M., H. B. Gray, and M. D. Hopkins. 1996. Electronic structure of metal-oxo complexes. In *Adv. in Trans. Met. Coord. Chem.*, ed. C.-M. Che and V. W.-W. Yam, 159. Vol. 1. Greenwich, CT: JAI Press.
42. Isovitsch, R. A., A. S. Beadle, F. R. Fronczek, and A. W. Maverick. 1998. Electronic absorption spectra and phosphorescence of oxygen-containing molybdenum(IV) complexes. *Inorg. Chem.*, 37, 4258.
43. Da Re, R. E., and M. D. Hopkins. 2002. Electronic spectra and structures of d^2 molybdenum-oxo complexes. Effects of structural distortions on orbital energies, two-electron terms, and the mixing of singlet and triplet states. *Inorg. Chem.*, 41, 6973.
44. Savoie, C., and C. Reber. 1998. Emitting state energies and vibronic structure in the luminescence spectra of *trans*-dioxorhenium(V) complexes. *Coord. Chem. Rev.*, 171, 387.
45. Savoie, C., and C. Reber. 2000. Coupled electronic states in trans-dioxo complexes of rhenium(V) and osmium(VI) probed by near-infrared and visible luminescence spectroscopy. *J. Am. Chem. Soc.*, 122, 844.
46. Kirgan, R. A., B. P. Sullivan, and D. P. Rillema. 2007. Photochemistry and photophysics of coordination compounds: Rhenium. *Top. Curr. Chem.*, 281, 45.
47. Lock, C. J. L., and G. Turner. 1978. A reinvestigation of dioxobis(ethylenediamine) rhenium(V) chloride and dioxotetrakis(pyridine)rhenium(V) chloride dihydrate. *Acta Cryst.*, B34, 923.
48. Bélanger, S., and A. L. Beauchamp. 1996. Preparation and protonation studies of *trans*-dioxorhenium(V) complexes with imidazoles. *Inorg. Chem.*, 35, 7836.
49. Grey, J. K., M. Triest, I. S. Butler, and C. Reber. 2001. Effect of pressure on the vibronic luminescence spectrum of a *trans*-dioxo rhenium(V) complex. *J. Phys. Chem. A*, 105, 6269.
50. Grey, J. K., I. S. Butler, and C. Reber. 2002. Effect of pressure on coupled electronic ground and excited states determined from luminescence spectra of *trans*-dioxorhenium(V) complexes. *J. Am. Chem. Soc.*, 124, 11699.
51. Grey, J. K., I. S. Butler, and C. Reber. 2004. Temperature- and pressure-dependent luminescence spectroscopy on the *trans*-$[ReO_2(pyridine)_4]^+$ complex—Analysis of vibronic structure, luminescence energies, and bonding characteristics. *Can. J. Chem.*, 82, 1083.
52. Newsham, M. D., E. P. Giannelis, T. J. Pinnavaia, and D. G. Nocera. 1988. The influence of guest-host interactions on the excited-state properties of dioxorhenium(V) ions in intracrystalline environments of complex-layered oxides. *J. Am. Chem. Soc.*, 110, 3885.
53. Grey, J. K., M. Marguerit, I. S. Butler, and C. Reber. 2002. Pressure-dependent Raman spectroscopy of metal-oxo multiple bonds in rhenium(V) and osmium(VI) complexes. *Chem. Phys. Lett.*, 366, 361.
54. Lanthier, E., J. Bendix, and C. Reber. 2010. Pressure-dependent luminescence spectroscopy of molybdenum(IV) oxo complexes. *Dalton Trans.*, 39, 3695.
55. Del Negro, A. S., Z. Wang, C. J. Seliskar, W. R. Heineman, B. P. Sullivan, S. E. Hightower, T. L. Hubler, and S. A. Bryan. 2005. Luminescence from the *trans*-dioxotechnetium(V) chromophore. *J. Am. Chem. Soc.*, 127, 14978.

56. Heines, P., H.-L. Keller, M. Armbrüster, U. Schwarz, and J. Tse. 2006. Pressure-induced internal redox reaction of $Cs_2[PdI_4]\cdot I_2$, $Cs_2[PdBr_4]\cdot I_2$, and $Cs_2[PdCl_4]\cdot I_2$. *Inorg. Chem.*, 45, 9818.
57. Allan, D. R., A. J. Blake, D. Huang, T. J. Prior, and M. Schröder. 2006. High pressure co-ordination chemistry of a palladium thioether complex: Pressure versus electrons. *Chem. Commun.*, 4081.
58. Abe, T., T. Itakura, N. Ikeda, and K. Shinozaki. 2009. Luminescence color change of a platinum(II) complex solid upon mechanical grinding. *Dalton Trans.*, 711.
59. Wenger, O. S., S. García-Revilla, H. U. Güdel, H. B. Gray, and R. Valiente. 2004. Pressure dependence of Pt(2,2′-bipyridine)Cl_2 luminescence. The red complex converts to a yellow form at 17.5 kbar. *Chem. Phys. Lett.*, 384, 190.
60. Grey, J. K., I. S. Butler, and C. Reber. 2003. Pressure-induced enhancements of luminescence intensities and lifetimes correlated with emitting-state distortions for thiocyanate and selenocyanate complexes of platinum(II) and palladium(II). *Inorg. Chem.*, 42, 6503.
61. Grey, J. K., I. S. Butler, and C. Reber. 2002. Large pressure-induced increase in luminescence intensity for the $[Pd(SCN)_4]^{2-}$ complex. *J. Am. Chem. Soc.*, 224, 9384.
62. Hidvegi, I., W. Tuszynski, and G. Gliemannn. 1981. Luminescence of $K_2Pt(SCN)_4$ single crystals at high pressure. *Chem. Phys. Lett.*, 77, 517.
63. Rohde, J.-U., B. von Malottki, and W. Preetz. 2000. Kristallstrukturen, spektroskopische Charakterisierung und Normalkoordinatenanalyse von $(n\text{-}Bu_4N)_2M(ECN)_4$. *Z. Anorg. Allg. Chem.*, 626, 905.
64. Pelletier, Y., and C. Reber. 2000. Luminescence spectroscopy and emitting-state properties of $Pd(SCN)_4^{2-}$ in crystals. *Inorg. Chem.*, 39, 4535.
65. Genre, C., G. Levasseur-Thériault, and C. Reber. 2009. Emitting-state properties of square-planar dithiocarbamate complexes of palladium(II) and platinum(II) probed by pressure-dependent luminescence spectroscopy. *Can. J. Chem.*, 87, 1625.
66. Levasseur-Thériault, G., C. Reber, C. Aronica, and D. Luneau. 2006. Large pressure-induced red shift of the luminescence band originating from nonstacked square-planar $[Pt(SCN)_4]^{2-}$ in a novel trimetallic complex. *Inorg. Chem.*, 45, 2379.
67. Pierce, E., E. Lanthier, C. Genre, Y. Chumakov, D. Luneau, and C. Reber. 2010. The Interaction of Thioether Groups at the Open Coordination Sites of Palladium(II) and Platinum(II) Complexes Probed by Luminescence Spectroscopy at Variable Pressure. *Inorg. Chem.*, 49, 4901.